Available online at www.sciencedirect.com
SCIENCE DIRECT
Journal of Catalysis 233 (2005) 109–118
JOURNAL OF CATALYSIS
www.elsevier.com/locate/jcat

Mathematical modeling of *o*-xylene hydrogenation kinetics over Pd/Al_2O_3

Henrik Backman [a], Ahmad Kalantar Neyestanaki [a,b], Dmitry Yu. Murzin [a,*]

[a] *Laboratory of Industrial Chemistry, Process Chemistry Centre, Åbo Akademi University, FIN-20500 Åbo/Turku, Finland*
[b] *Nynäs Naphthenics AB, SE-149 82, Nynäshamn, Sweden*

Received 17 February 2005; revised 15 April 2005; accepted 24 April 2005

Available online 23 May 2005

Abstract

A mechanistic model of surface reactions has been developed to describe the kinetic behavior and the stereochemical product distribution for the gas-phase hydrogenation of *o*-xylene over Pd/Al_2O_3. Models considering competitive, noncompetitive, and semicompetitive adsorption between hydrogen and *o*-xylene, featuring stepwise and pairwise addition of hydrogen atoms to the adsorbed *o*-xylene molecule, were applied. The stereochemical distribution of the products (*cis*- and *trans*-dimethylcyclohexane) was determined by the surface behavior of a cyclic olefin (reaction intermediate). This olefin is either directly hydrogenated to *cis*-DMCH or hydrogenated via a rollover mechanism to *trans*-DMCH. The stereochemical distribution was dependent on both temperature and the partial pressures of the reactants, which was explained by the advanced mathematical model. The model considering competitive adsorption turned out to better explain the stereochemical product distribution than the noncompetitive model. An extension of the competitive model, for example, the semicompetitive model, which allowed hydrogen to adsorb between adsorbed organic molecules, was also capable of explaining the main kinetic regularities, although with a slightly lower accuracy for the estimated parameters.

Keywords: *o*-Xylene; Hydrogenation; Kinetic modeling

1. Introduction

The hydrogenation of aromatics has been investigated intensively for decades because of its industrial and theoretical importance. Traditionally benzene has been the most used model reactant, but more recently other model components have been applied, such as toluene and xylenes. Gas-phase hydrogenation of aromatics is generally carried out over different supported Pd, Ni, and Pt catalysts [1–13]. The hydrogenation of aromatic components is also of interest because of more stringent environmental legislation, as the removal of aromatic components is beneficial for the quality of diesel fuel. In particular, the cetane number increases with decreasing aromatic content. Hydrogenation of benzene, in addition, is widely used as a probe reaction to test the hydrogenation functionality of metal catalysts.

Various kinetic models have been proposed to understand the kinetics of the hydrogenation of aromatics. Models taking into account the stereochemistry are more sparsely reported, and, furthermore, few are applicable over a wide range of reaction conditions. Concerning the hydrogenation of the aromatic ring in general, there is a controversy about the mechanism, mainly with respect to the nature of the active sites and the adsorption of hydrogen and aromatics. Some researchers propose that hydrogen is added as single hydrogen atoms, and others suggest that hydrogen is added in molecular form to the aromatic molecule. There are also differences of opinion over whether the adsorption of the aromatic molecule and hydrogen molecule is competitive or noncompetitive. Most kinetic models assume a sequence of hydrogen addition steps.

* Corresponding author. Fax: +358 2 2154479.
E-mail address: dmurzin@abo.fi (D.Yu. Murzin).

0021-9517/$ – see front matter
doi:10.1016/j.jcat.2005.04.029

The addition of the first hydrogen atom to the aromatic ring has been proposed to be the rate-determining step in benzene and toluene hydrogenation [14], because the aromaticity is broken when the first hydrogen is added. Mechanistic considerations of [4–6,15] were inspired by earlier studies on liquid-phase hydrogenation of benzene and substituted aromatics, where a kinetic model, consistent with thermodynamics, was advanced [15,16]. Other studies have also proposed a kinetic model without a single rate-determining step [17,18]. A noncompetitive Langmuir–Hinshelwood mechanism has also been proposed for the gas-phase hydrogenation of *o*-xylene over alumina-supported platinum catalyst [11].

With regard to stereoselectivity, Smeds et al. [4–6] investigated gas-phase hydrogenation of alkylaromatics and derived a kinetic model in which a cyclic olefin was a precursor in the formation of *cis*- and *trans*-dimethylcyclohexanes. Their mechanism took into account a concept of Siegel et al. [19], where the stereoselectivity is governed by desorption and readsorption of the cyclic olefin. Viniegra et al., on the other hand, proposed that the stereoselectivity is a result of a "rollover" process of the surface intermediate [1]. A comparison was made between rollover and desorption–readsorption mechanisms in [20].

The aim of this work is to present a mechanism that describes the kinetics and stereoselectivity of gas-phase hydrogenation of *o*-xylene over Pd/Al_2O_3. The experimental description was published earlier [21].

2. Experimental

Gas-phase hydrogenation of *o*-xylene was studied in a differential tube reactor at a WHSV of 70 h^{-1} and in the temperature range of 440–520 K with 10 K intervals at atmospheric pressure. The partial pressures of hydrogen and *o*-xylene were varied between 0.24–0.61 and 0.0612–0.612 bar, respectively. Argon was used as the makeup gas. Liquid *o*-xylene was fed to the reactor through an evaporator by an HPLC pump, and a Varian GC was used to analyze the reaction products. The 1% Pd-alumina catalyst was prepared by impregnation of a γ-alumina support (BET 249 m^2/g) with a solution of pre-acidified $PdCl_2$. More detailed information about the experimental setup and the catalyst can be found in [21].

2.1. *o*-Xylene hydrogenation

cis- and *trans*-1,2-dimethylcyclohexane (1,2-DMCH) were the only hydrogenation products (i.e., no dimethylcyclohexene or dimethylcyclohexadiene was detected). As in benzene and toluene hydrogenation, the reaction rate for xylene hydrogenation passes through a maximum at approximately 490 K. The reaction orders with respect to hydrogen increased with temperature from 1.3 at 440 K to 2.6 at 520 K, similar to previously observed hydrogen concentration dependencies over supported Ni/Al_2O_3 and Pt/Al_2O_3 catalysts. The reaction orders with respect to *o*-xylene were found to be slightly negative (~ -0.2) at all temperatures investigated. The results indicated that the formation of *trans*-isomer was favored by increased reaction temperature but decreased with increased hydrogen partial pressure. The changes in *o*-xylene partial pressure altered the *cis*/*trans* ratio to a small extent. It should also be pointed out that the initial deactivation of the catalyst did not affect the stereoselectivities. The dependency of stereoselectivity on the operation temperature and reactant concentrations is in good agreement with previous works on supported metal catalysts [4,22].

3. Results and discussion

3.1. Descriptive kinetics of stereoselectivity

Hydrogenation of *o*-xylene involves the destruction of the ring structure in the aromatic molecule. Stepwise addition of a hydrogen atom (molecular or atomic) to the aromatic molecule has been suggested to be the dominating mechanism, since this reaction probability is higher than that for simultaneous multiple additions of hydrogen atoms. Saeys et al. [23,24] have reported that there is a strong indication of a dominant reaction path for benzene hydrogenation over a Pt(111) catalyst, which follows the classical Horiuti–Polanyi mechanism involving consecutive addition of hydrogen, where the only reaction product is cyclohexane. According to the study of Sayes et al. the reaction path does not pass through cyclohexadiene or cyclohexene, which is in agreement with the thermodynamic considerations [16]. Smeds et al. suggested, in their study of hydrogenation of *o*- and *p*-xylene over Pt-alumina, a mechanistic scheme in which the aromatic character remains during the first two hydrogen addition steps, which is in line with the aromaticity principle proposed by Temkin for benzene hydrogenation [25]. A more detailed discussion of the nature of this intermediate with respect to the thermodynamics can be found in papers by Smeds et al. [5,26].

Benzene, toluene, and *o*-xylene are believed to adsorb parallel to the surface of group VIII metals because of the interaction between π-electrons in the aromatic ring and the unoccupied *d*-metal orbitals [27,28]. To reduce the repulsive effect, the two methyl substituents in *o*-xylene should be oriented away from the surface, and consequently *cis*-DMCH should be the product formed from 1,2-dimethylcyclohexene (Scheme 1). Hence, the *cis* stereoisomer is the kinetically favored product. Several scientists have previously reported a higher selectivity for the thermodynamically more stable *trans* isomer with increasing temperature.

The increase in the formation of *trans*-1,2-DMCH as a result of higher temperature is generally explained by the rollover mechanism, first introduced by Inuone et al. [29],

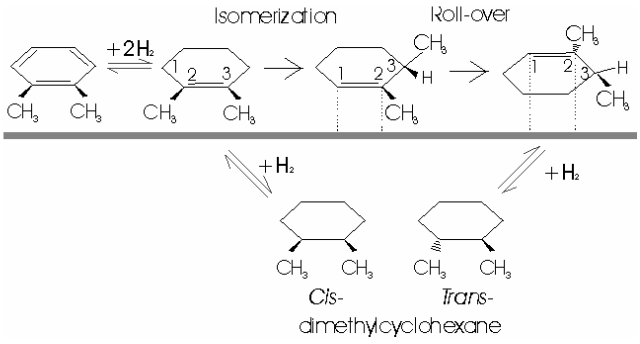

Scheme 1. Formation of *cis*- and *trans*-dimethylcyclohexane.

with the assumption that the last double bond to be hydrogenated is isomerized, followed by rollover of the adsorbed species, the hydrogenation of which results in *trans*-1,2-DMCH. The rollover mechanism is presented in Scheme 1, according to which 1,2-dimethylcyclohexene is isomerized to 2,3-dimethylcyclohexene and subsequently rolls over, leading to formation of the *trans* isomer by hydrogenation of the last double bond. The rate of formation of *trans*-1,2-DMCH is hereby determined by the relative ratio of 1,2-dimethylcyclohexene (DMCHe) hydrogenation and isomerization. At lower temperatures the *cis*-1,2-DMCH is the dominant reaction product, whereas the formation of the thermodynamically favored *trans*-1,2-DMCH is increased by increased operation temperature. The *cis*/*trans* ratio also increases with increasing partial pressure of hydrogen, which, on the other hand, results in a higher reaction rate. More detailed information about stereoselectivity dependence on reaction parameters in *o*-xylene hydrogenation can be found in [21].

In the past the mathematical approach to heterogeneous catalytic kinetics was to formulate models that could be solved analytically, because of limited computational capacity. Often purely empirical models, such as power-law models, were used (and are still frequently used) to describe the rate of the reactions, resulting in not very realistic models with limited predictive abilities. The increase in computational power has led to more complex kinetic models involving elementary reactions that make the process better understood. In combination with reliable data from kinetic measurements and surface science studies, advanced mathematical modeling provides a powerful tool for both scientists and engineers. Reaction kinetics is the translation of our understanding of the chemical process into a mathematical rate expression that can be also used in reliable and predictive reactor design [30]. The goal of mathematical analysis is, in a way, the understanding of the process rather than only the estimation of the values of the parameters.

The mechanism of *o*-xylene hydrogenation can be written in the case of noncompetitive adsorption in the following way with two reaction routes, $N^{(1)}$ and $N^{(2)}$, for the formation of, respectively, *cis*- and *trans*-dimethylcyclohexane:

	$N^{(1)}$	$N^{(2)}$
$S + A \equiv AS$	1	1
$j^* + H_2 \equiv jH^*_{2/j}$	1	1
1. $AS + jH^*_{2/j} \rightleftharpoons AH_2S + j^*$	1	1
2. $AH_2S + jH^*_{2/j} \rightleftharpoons AH_4S + j^*$	1	1
3. $AH_4S \rightarrow OS$	1	1
4. $OS + jH^*_{2/j} \rightarrow C + S + j^*$	1	0
5. $OS \rightleftharpoons O'S$	0	1
6. $O'S + jH^*_{2/j} \rightarrow T + S + j^*$	0	1

$N^{(1)},\ A + 3H_2 = C;\ N^{(2)},\ A + 3H_2 = T.$ (1)

Here S represents the adsorption site for the aromatic species; * is a surface adsorption site for hydrogen; j equals 1 for molecular hydrogen adsorption and 2 for dissociative adsorption; *o*-xylene and hydrogen are denoted by A and H, respectively; C and T are respectively *cis*- and *trans*-1,2-DMCH; and O and AH_4 represent respectively 1,2-dimethylcyclohexene and a surface intermediate, which still retains its aromatic character. AH_4 is the precursor of the intermediate O, which can undergo either hydrogenation to *cis*-1,2-DMCH (step 4) or isomerization (described by step 5) of 1,2-DMCHe and rollover of the intermediate 1,3-DMCHe. The overall reactions are obtained by a combination of the chemical equations multiplied by the stoichiometric numbers.

For competitive adsorption the mechanism can be written as

	$N^{(1)}$	$N^{(2)}$
$x^* + A \equiv xA^*$	1	1
$j^* + H_2 \equiv jH^*_{2/j}$	1	1
1. $xA^* + jH^*_{2/j} \rightleftharpoons xAH^*_2 + j^*$	1	1
2. $xAH^*_2 + jH^*_{2/j} \rightleftharpoons xAH^*_4 + j^*$	1	1
3. $xAH^*_4 \rightarrow xO^*$	1	1
4. $xO^* + jH^*_{2/j} \rightarrow C + j^* + x^*$	1	0
5. $xO^* \rightleftharpoons xO'^*$	0	1
6. $xO'^* + jH^*_{2/j} \rightarrow T + j^* + x^*$	0	1

$N^{(1)},\ A + 3H_2 = C;\ N^{(2)},\ A + 3H_2 = T.$ (2)

Here * denotes an active site for both hydrogen and the aromatic molecule; x is the number of *-sites covered by the *o*-xylene molecule. Our observation of decreasing reaction rate with increasing partial pressure of *o*-xylene could be an indication that the *o*-xylene molecules block the active sites, resulting in a decreased reaction rate. It is commonly assumed that the number of adsorption sites on which an organic molecule is adsorbed is equal to unity. This is a simplification, however, since it neglects the polyatomic nature of the reacting molecule. Hydrocarbons are thought to require several sites for adsorption, whereas hydrogen is adsorbed on only a single metal site, resulting in competition for sites between participating molecules [30,31]. The diameter of the *o*-xylene molecule is about 5.8 Å, whereas that of the hydrogen molecule is 0.7 Å. Since the *o*-xylene molecule is much larger than the hydrogen molecule and the distance

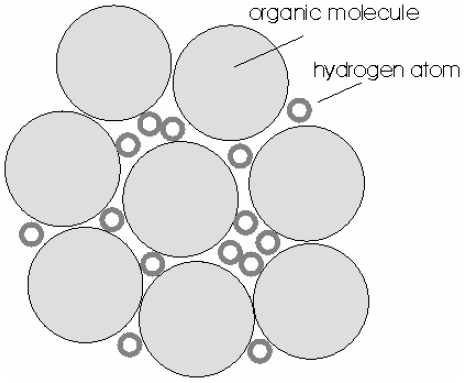

Fig. 1. Adsorption of hydrogen on interstitial sites between larger molecules.

between the Pd atoms is ∼ 2.7 Å (if a Pd(111) surface is considered), *o*-xylene can possibly cover up to seven sites. The molecule structure was optimized with the Universal Force Field (UFF 1.02) as implemented in Cerius^2 (Version 4.8; Accelrys Inc.). (Note that if the Connolly surface were to be taken into consideration, the length of *o*-xylene would be calculated to be 8.0 Å for a probe radius of 1.4 Å.)

The cases of competitive and noncompetitive adsorption are extreme, and the true nature lies most probably somewhere in between. Frennet et al. have demonstrated that on a Rh surface adsorbed to saturation with methane, a further amount of hydrogen can be adsorbed on the surface [32]. When no more free sites are available for the adsorption of molecules that are large compared with the size of the adsorption site, the hindered sites may still be free for small molecules like hydrogen (Fig. 1). If two types of sites are considered, one type of site can be occupied by both components, whereas the other type can be occupied by only one of the components. The second component is excluded from the first type of site for two possible reasons: size exclusion or lack of competition. The size exclusion can easily be understood geometrically if the metal surface is modeled with a sheet of squared paper, where one square is an adsorption site, and the organic molecules proportional to the squares are placed on this paper. The organic molecules will not be able to completely cover the surface and in the spaces between the larger molecules, the smaller hydrogen atoms are assumed to be able to adsorb.

The concept of multicentered adsorption has also been verified experimentally for the adsorption of aromatics [33]. Mikkola et al. [34] proposed for liquid-phase hydrogenation of xylose to xylitol, a semicompetitive model based on the hypothesis that organic molecules occupy several primary sites for the adsorption of a hydrogen molecule. An assumption that the organic molecule is not able to completely cover the catalyst surface was also introduced. The smaller hydrogen atoms are able to adsorb on the interstitial sites between the larger molecules. Even though the model allows for competitive adsorption, there is always a fraction of the total surface area accessible for noncompetitive hydrogen adsorption (Fig. 1). It was assumed that the total number of hydrogen sites in the balance equation includes organic sites. In the present study the concept of semicompetitive adsorption was tested with *o*-xylene hydrogenation data.

3.2. Derivation of rate equations

Quasiequilibrium approximation is assumed for the adsorption of the reactants

$$K_{\mathrm{H}} = \frac{\theta_{\mathrm{H}}^{j}}{P_{\mathrm{H}}\theta_{*}^{j}}, \tag{3}$$

$$K_{\mathrm{A}} = \frac{\theta_{\mathrm{A}}}{P_{\mathrm{A}}\theta_{*}^{X}} \quad \text{(competitive adsorption)} \quad \text{or} \tag{4}$$

$$K_{\mathrm{A}} = \frac{\theta_{\mathrm{A}}}{P_{\mathrm{A}}\theta_{\mathrm{s}}} \quad \text{(non-competitive adsorption)}. \tag{5}$$

The steady-state hypothesis gives for the surface reaction steps

$$r = r_1 = r_2 = r_3 = r_4 + r_6, \qquad r_5 = r_6, \tag{6}$$

where

$$\begin{aligned} r_1 &= k_1\theta_{\mathrm{A}}\theta_{\mathrm{H}}^{j} - k_{-1}\theta_{\mathrm{AH_2}}\theta_{*}^{j},\\ r_2 &= k_2\theta_{\mathrm{AH_2}}\theta_{\mathrm{H}}^{j} - k_{-2}\theta_{\mathrm{AH_4}}\theta_{*}^{j},\\ r_3 &= k_3\theta_{\mathrm{AH_4}},\\ r_4 &= k_4\theta_{\mathrm{O}}\theta_{\mathrm{H}}^{j},\\ r_5 &= k_5\theta_{\mathrm{O}} - k_{-5}\theta_{\mathrm{O'}},\\ r_6 &= k_6\theta_{\mathrm{O'}}\theta_{\mathrm{H}}^{j}. \end{aligned} \tag{7}$$

A combination of reactions (1)–(3),

$$\begin{cases} k_1\theta_{\mathrm{A}}\theta_{\mathrm{H}} - k_{-1}\theta_{\mathrm{AH_2}}\theta_{*} = k_2\theta_{\mathrm{AH_2}}\theta_{\mathrm{H}} - k_{-2}\theta_{\mathrm{AH_4}}\theta_{*},\\ k_2\theta_{\mathrm{AH_2}}\theta_{\mathrm{H}} - k_{-2}\theta_{\mathrm{AH_4}}\theta_{*} = k_3\theta_{\mathrm{AH_4}}, \end{cases} \tag{8}$$

gives the surface coverage of AH_4

$$\theta_{\mathrm{AH_4}} = \frac{k_1k_2\theta_{\mathrm{H}}^{2j}\theta_{\mathrm{A}}}{k_2k_3\theta_{\mathrm{H}}^{j} + k_3k_{-1}\theta_{*}^{j} + k_{-1}k_{-2}\theta_{*}^{2j}}. \tag{9}$$

After insertion of Eq. (9) into Eq. (7) (step 3), the rate can be written as

$$r_3 = \frac{k_3\frac{k_1k_2(K_{\mathrm{H}}P_{\mathrm{H}})^2\theta_{\mathrm{A}}}{k_{-1}k_{-2}}}{1 + \frac{k_3}{k_{-2}\theta_{*}^{j}} + \frac{k_2k_3K_{\mathrm{H}}P_{\mathrm{H}}}{k_{-1}k_{-2}\theta_{*}^{j}}}. \tag{10}$$

In Eq. (10) θ_{A} is calculated from Eqs. (4) or (5), depending on whether it is a competitive or noncompetitive adsorption.

The stereochemistry for *o*-xylene is dependent on both temperature and the reactant pressure, and, therefore, the intermediates O and O′ are not bound by an equilibrium, as elaborated by Smeds et al. [6]. The ratio between θ_{O} and $\theta_{\mathrm{O'}}$ determines the stereochemical distribution and the pressure dependency

$$\frac{r_{cis}}{r_{trans}} = \frac{k_4\theta_{\mathrm{O}}}{k_6\theta_{\mathrm{O'}}} = \frac{k_4(k_{-5} + k_6\theta_{\mathrm{H}}^{j})}{k_5k_6}, \tag{11}$$

where θ_{Olefin} is calculated from

$$k_5\theta_{\text{O}} - k_{-5}\theta_{\text{O}'} = k_6\theta_{\text{O}'}\theta_{\text{H}}, \tag{12}$$

$$\theta_{\text{O}} = \left(\frac{k_{-5} + k_6\theta_{\text{H}}^j}{k_5}\right)\theta_{\text{O}'}. \tag{13}$$

The decrease in selectivity to the *trans* isomer with increasing partial pressure of hydrogen, and consequently hydrogen coverage, explicitly follows from Eq. (11) in accordance with experimental data. The experimental data showed that the partial pressure of *o*-xylene altered the *cis*/*trans* ratio, but to a small extent. This behavior is not directly seen in Eq. (11) but could be explained, however, by this equation, since implicit dependence of the *cis*/*trans* ratio on *o*-xylene coverage follows from its dependence on hydrogen coverage in the case of competitive adsorption.

The sum of the surface coverages for the same type of surface site is equal to unity, which results in the following balance equations for noncompetitive adsorption

$$\begin{cases} \theta_{\text{A}} + \theta_{\text{AH}_2} + \theta_{\text{AH}_4} + \theta_{\text{O}} + \theta_{\text{O}'} + \theta_{\text{S}} = 1, \\ \theta_{\text{H}} + \theta_* = 1. \end{cases} \tag{14}$$

The coverage of hydrogen (θ_{H}) is most conveniently calculated from Eq. (3), which gives for the coverage of free sites for hydrogen adsorption

$$\theta_* = \frac{1}{1 + (K_{\text{H}}P_{\text{H}})^{1/j}}. \tag{15}$$

After elimination of the surface coverages, the rate equation, in the case of noncompetitive adsorption, can be written as

$$r = k_3\frac{k_1k_2(K_{\text{H}}P_{\text{H}})^2}{k_{-1}k_{-2}} \Bigg/ \Bigg[(1 + K_{\text{A}}P_{\text{A}}a)\left(1 + \frac{k_3(1 + (K_{\text{H}}P_{\text{H}}))^{1/j}}{k_{-2}} + \frac{k_2k_3K_{\text{H}}P_{\text{H}}(1 + (K_{\text{H}}P_{\text{H}})^{1/j})}{k_{-1}k_{-2}}\right)\Bigg], \tag{16}$$

where

$$a = 1 + \frac{k_1K_{\text{H}}p_{\text{H}}\theta_*^j}{k_{-1}\theta_*^j + \frac{k_2k_3K_{\text{H}}p_{\text{H}}\theta_*^j}{k_{-2}\theta_*^j + k_3}} + \left(\frac{k_2K_{\text{H}}p_{\text{H}}\theta_*^j}{k_{-2}\theta_*^j + k_3}\right)\left(\frac{k_1K_{\text{H}}p_{\text{H}}\theta_*^j}{k_{-1}\theta_*^j + \frac{k_2k_3K_{\text{H}}p_{\text{H}}\theta_*^j}{k_{-2}\theta_*^j + k_3}}\right) + k_1k_3K_{\text{H}}p_{\text{H}}\theta_*^j \Bigg/ \Bigg[\left(k_4\left(\frac{k_{-5} + k_6\theta_{\text{H}}^j}{k_5}\right) + k_6K_{\text{H}}p_{\text{H}}\theta_*^j\right) \times \left(k_{-1}\theta_*^j + \frac{k_2k_3K_{\text{H}}p_{\text{H}}\theta_*^j}{k_{-2}\theta_*^j + k_3}\right)\Bigg] \times \left(1 + \left(\frac{k_{-5} + k_6\theta_{\text{H}}^j}{k_5}\right)\right). \tag{17}$$

θ_{H} and θ_* are given by Eqs. (3) and (12), respectively.

For competitive adsorption the balance equation is

$$\theta_{\text{H}} + x(\theta_{\text{A}} + \theta_{\text{AH}_2} + \theta_{\text{AH}_4} + \theta_{\text{O}} + \theta_{\text{O}'}) + \theta_* = 1, \tag{18}$$

where θ_{H} and θ_{A} are calculated from Eqs. (3) and (4), respectively. θ_{AH_2} can be derived in the same way as θ_{AH_4} [Eqs. (8) and (9)], whereas θ_{O} and $\theta_{\text{O}'}$ can be calculated from Eqs. (12) and (13). Insertion in Eq. (15) gives

$$K_{\text{H}}P_{\text{H}} + xK_{\text{A}}P_{\text{A}}\theta_*^x + \frac{k_1K_{\text{H}}P_{\text{H}}\theta_*^j}{k_{-1}\theta_*^j + \frac{k_2k_3K_{\text{H}}P_{\text{H}}\theta_*^j}{k_{-2}\theta_*^j + k_3}}xK_{\text{A}}P_{\text{A}}\theta_*^X + \frac{k_2K_{\text{H}}P_{\text{H}}\theta_*^j}{k_{-2}\theta_*^j + k_3}\frac{k_1K_{\text{H}}P_{\text{H}}\theta_*^j}{k_{-1}\theta_*^j + \frac{k_2k_3K_{\text{H}}P_{\text{H}}\theta_*^j}{k_{-2}\theta_*^j + k_3}}xK_{\text{A}}P_{\text{A}}\theta_*^X + \left(\frac{k_{-5} + k_6\theta_{\text{H}}^j}{k_5} + 1\right)k_1k_3K_{\text{H}}P_{\text{H}}xK_{\text{A}}P_{\text{A}}\theta_*^j\theta_*^X \Bigg/ \Bigg[\left(k_4\left(\frac{k_{-5} + k_6\theta_{\text{H}}^j}{k_5}\right) + k_6K_{\text{H}}P_{\text{H}}\theta_*^j\right) \times \left(k_{-1}\theta_*^j + \frac{k_2k_3K_{\text{H}}P_{\text{H}}\theta_*^j}{k_{-2}\theta_*^j + k_3}\right)\Bigg] + \theta_* = 1. \tag{19}$$

In the case of competitive adsorption θ_* can only be solved numerically. The solution of θ_* is then inserted into Eq. (10).

The semicompetitive model is based on the assumption that the organic molecule can occupy several sites. It is also assumed that the organic molecule is not able to completely cover the catalyst surface. The site balances for hydrogen and organic species can be written as

$$\theta_{\text{S}} + x(\theta_{\text{A}} + \theta_{\text{AH}_2} + \theta_{\text{AH}_4} + \theta_{\text{O}} + \theta_{\text{O}'}) + (K_{\text{H}}P_{\text{H}})^{1/j}\theta_{\text{S}} = \alpha, \tag{20}$$

$$\theta_* = \theta_{\text{S}} + x(\theta_{\text{A}} + \theta_{\text{AH}_2} + \theta_{\text{AH}_4} + \theta_{\text{O}} + \theta_{\text{O}'})(1 - \alpha), \tag{21}$$

$$\theta_* + (K_{\text{H}}P_{\text{H}})^{1/j}\theta_* + x(\theta_{\text{A}} + \theta_{\text{AH}_2} + \theta_{\text{AH}_4} + \theta_{\text{O}} + \theta_{\text{O}'}) = 1. \tag{22}$$

Here α gives the coverage of adsorption sites for the organic species on the surface, whereas the free sites for hydrogen adsorption are denoted by θ_*. The competitive model is then just a special case of the semicompetitive model, since for $\alpha = 1$ we get the case with full competition between hydrogen and the organic species.

After combination the coverage of free sites for hydrogen adsorption can be expressed as

$$\theta_* = \frac{1}{(K_{\text{H}}P_{\text{H}})^{1/j} + \frac{1 + K_{\text{A}}P_{\text{A}}a}{1 + (1-\alpha)(K_{\text{A}}P_{\text{A}}a)}}, \tag{23}$$

where a is taken from Eq. (17). Eq. (23) is the same as Eq. (15) if α is equal to zero, which means that we end up with a model that is similar to the noncompetitive model. Consequently, α should have a value between 0 and 1 if semicompetitive adsorption takes place.

An Arrhenius type of temperature dependence was used for the rate constants:

$$k_i = k(T)\text{e}^{-\frac{E}{R}\left(\frac{1}{T} - \frac{1}{\overline{T}}\right)}, \tag{24}$$

where $\overline{T}$ is the average temperature.

For the temperature dependence of the equilibrium constants, the van't Hoff equation was applied

$$K_i = \mathrm{e}^{\frac{\Delta S_i}{R}} \mathrm{e}^{\frac{-\Delta H_i}{RT}}, \tag{25}$$

where ΔS is adsorption entropy and ΔH is the adsorption enthalpy.

The coverages are most conveniently calculated numerically by the Newton–Raphson method or the Secant method [35]. The Secant method requires only evaluation of $f(x)$ and is almost as fast as the Newton method, which involves evaluation of the derivative $f'(x)$. The Secant method is used in the present study for the numerical solution of the model for competitive and semicompetitive adsorption.

3.3. Parameter estimation

The kinetic models were fitted by nonlinear regression analysis against the experimental data. We obtained the model predictions by solving the algebraic equations for the surface coverages during the parameter estimation, using the parameter estimation software ModEst 6.0 [36]. A combined simplex-Levenberg–Marquardt algorithm implemented in the software was used to minimize the residual sum of squares between experimental and calculated reaction rates. The most common measure for the goodness of fit is the R^2 value, given by the expression

$$R^2 = 100\left(1 - \frac{\|c_{\mathrm{exp}} - c_{\mathrm{est}}\|^2}{\|c_{\mathrm{exp}} - \bar{c}_{\mathrm{exp}}\|^2}\right), \tag{26}$$

where the values c_{est} denote the predictions given by the model and $\bar{c}_{\mathrm{exp}}$ is the mean value of all the data points.

The generation rates were calculated from the mass balances of a differential reactor, where the molar flow of the product was obtained from the total flow through the reactor and the measured mole fraction of the product

$$r_i = \frac{p_i F_{\mathrm{tot}}}{p_{\mathrm{tot}} m_{\mathrm{metal}}}. \tag{27}$$

The partial pressures were varied between 0.61 and 0.061 bar for hydrogen and 0.061 and 0.123 bar for *o*-xylene, giving eight data points at each temperature. The temperature range was 440–520 K (10 K intervals). Hence, the total number of experimental observations was around 72, giving a degree of freedom of 48. The reproducibility of the results was ±2%. A minor time-on-stream catalyst deactivation took place during the first 20 min. The deactivation was believed to be a result of carbon deposition [37]. Since the first experimental observation was made after 5 min of reaction, a mechanistic deactivation model [38] was applied to obtain the initial rates used in the kinetic calculations. In Fig. 2, r represents the reaction rate, t is the time on stream, and a_1–a_3 are the rate constants for deactivation and self-regeneration. The reaction rate at a time infinitely close to zero can be expressed by the sum of a_1 and a_3. The model satisfactorily describes the deactivation of the catalyst.

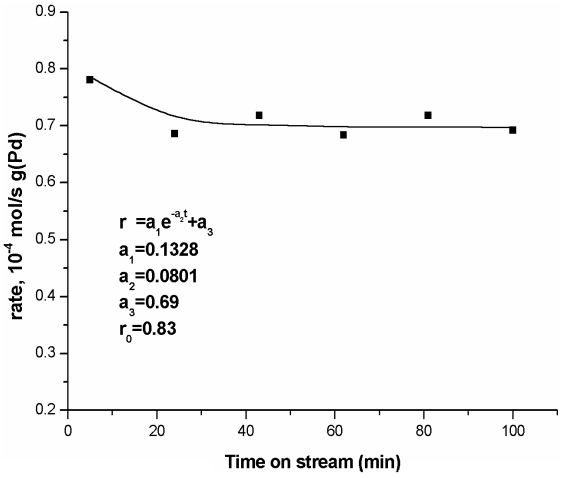

Fig. 2. Time-on-stream deactivation at 500 K. (●) observed rate, (—) calculated rate. $p_{\mathrm{H_2}} = 0.61$ bar, $p_{o\text{-xyl}} = 0.061$ bar.

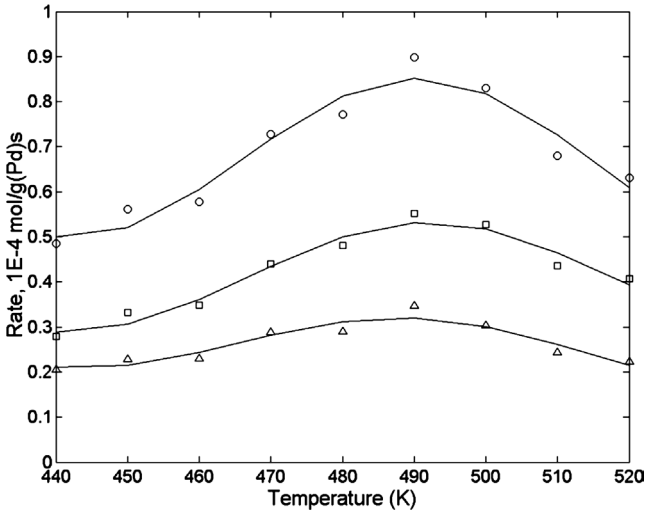

Fig. 3. Hydrogenation of *o*-xylene over Pd/Al_2O_3 440–520 K. Total hydrogenation rate (○) r_{trans} (□) and r_{cis} (Δ). Initial rates. $p_{\mathrm{H_2}} = 0.6$ bar, $p_{\mathrm{A}} = 0.061$ bar. Competitive model and dissociative hydrogen adsorption. Degree of explanation, 98.4%.

Models describing noncompetitive, competitive, and semicompetitive adsorption, as well as dissociative and nondissociative hydrogen adsorption, were tested against the experimental data. It turned out, however, that, in contrast to competitive adsorption (Figs. 3 and 4) and semicompetitive adsorption, the noncompetitive model was not able to describe the sharp temperature dependency in the hydrogenation rate sufficiently well. Furthermore, the change in the *cis*/*trans* ratio that occurred with the change in the partial pressure of *o*-xylene could not be explained within reasonable values of the estimated parameters. The competitive and semicompetitive models, on the other hand, could predict this observed dependence (Fig. 5). The explanation for this could be that in competitive adsorption the partial pressure of *o*-xylene affects the coverage of hydrogen. The increase in *o*-xylene partial pressure reduced the concentration of

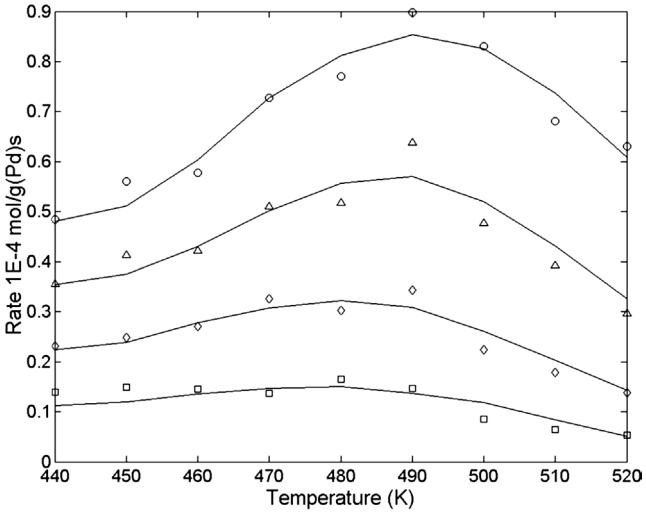

Fig. 4. Hydrogenation rate at different partial pressures of hydrogen (p_{H_2} = 0.61 (○), 0.49 (Δ), 0.36 (◇), 0.24 bar (□), p_A = 0.061 bar). Competitive adsorption and dissociative hydrogen adsorption.

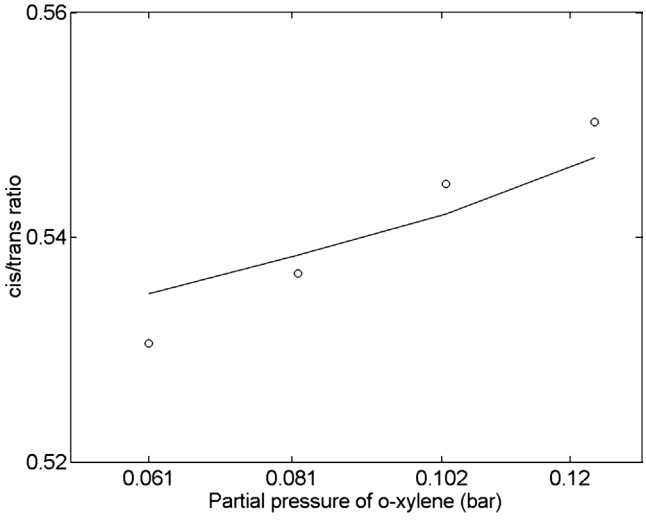

Fig. 5. *cis*/*trans* ratio at 510 K. p_{H_2} = 0.61. p_A = 0.061–0.123 bar. Model of competitive and dissociative hydrogen adsorption.

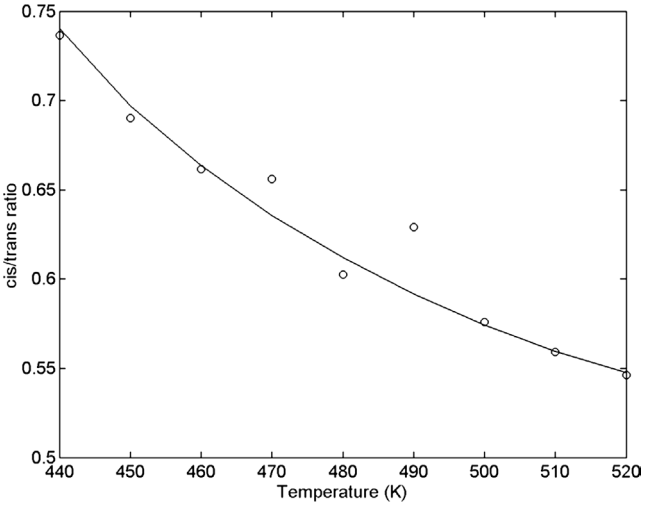

Fig. 6. *cis*/*trans* ratio as a function of temperature. p_{H_2} = 0.61 bar, p_A = 0.06 bar. Model of semicompetitive and dissociative hydrogen adsorption.

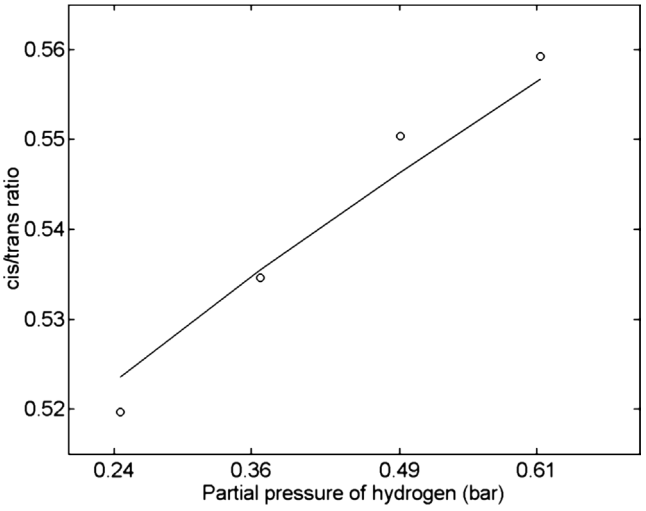

Fig. 7. *cis*/*trans* as a function of partial pressure of hydrogen at 510 K. p_A = 0.061. Model of competitive and dissociative hydrogen adsorption.

hydrogen on the surface of the catalyst, which, according to Eq. (23), raises the *cis*/*trans* ratio. The increased partial pressure of *o*-xylene should lead, as well, to a decrease in the total hydrogenation rate as experimentally observed. Although the change in the *cis*/*trans* ratio with changing *o*-xylene pressure was small, it could not be neglected. Competitive adsorption of the aromatic molecule and hydrogen has been assumed previously in benzene and toluene hydrogenation [39,40].

The ability of the competitive model to describe the kinetic behavior is illustrated in Figs. 3 and 4. The model describing the observed kinetics in the best way is the variant with dissociative hydrogen adsorption. The stereochemistry as a function of temperature and as a function of the partial pressure of hydrogen is well predicted by this model, as shown in Figs. 6 and 7. The calculated parameters for the competitive adsorption model are presented in Table 1.

The semicompetitive model did not further improve the fit of the model to the experimental data, but it gives, however, an interesting indication of the coverage on the catalyst surface, since α, the coverage of the organic species, was calculated to be around 0.6 (see Table 1), which means that the large organic molecule is not able to completely cover the surface of the catalyst because of geometric restrictions. Note that the value of α is close to the total surface coverage calculated by Snagovskii for the adsorption of aromatics within the framework of the shielding model [41]. The estimated parameters, presented in Table 1, were not as well defined as the parameters estimated for the competitive model, which could be caused by the fact that the semicompetitive model is more complicated than both the noncompetitive and competitive models. Some differences between competitive and semicompetitive models could be

Table 1
Estimated parameters for the models

	Competitive adsorption		Semicompetitive adsorption	
	Non-dissociative H_2 adsorption	Dissociative H_2 adsorption	Non-dissociative H_2 adsorption	Dissociative H_2 adsorption
Degree of explanation	97.7%	98.4%	97.6%	98.1%
Residual SS Q	0.035	0.021	0.0268	0.032
k_1	0.3 ± 0.15	0.5 ± 0.3	$0.3 \pm \ldots$	0.2 ± 0.5
E_{a_1}	121 ± 23.1	116 ± 12.2	117 ± 27	121 ± 19.1
k_{-1}	$3.1 \pm \ldots$	0.8 ± 0.4	0.8 ± 0.5	$0.7 \pm \ldots$
$E_{a_{-1}}$	145 ± 37.2	$126 \pm \ldots$	127 ± 12	123 ± 52.5
k_2	0.4 ± 0.07	0.7 ± 0.3	$0.2 \pm \ldots$	0.1 ± 0.2
E_{a_2}	135 ± 16.2	124 ± 7.2	125 ± 66.1	131 ± 42.1
k_{-2}	7.7 ± 1.8	0.9 ± 0.1	1.3 ± 1.1	1.4 ± 0.9
$E_{a_{-2}}$	147 ± 28.2	143 ± 52.8	135 ± 25.1	140 ± 62
k_3	$4.8 \pm \ldots$	$3.9 \pm \ldots$	5.8 ± 4.7	$3.6 \pm \ldots$
E_{a_3}	76.7 ± 42.2	64.8 ± 27.3	$65.1 \pm \ldots$	60.2 ± 49.7
k_4	17.2 ± 1.3	13.5 ± 7.3	11 ± 2.2	$15.1 \pm \ldots$
E_{a_4}	72.1 ± 40.2	70.7 ± 11.6	75.1 ± 18	79 ± 22.3
k_5	5.5 ± 1.7	5.5 ± 0.9	8.1 ± 7.2	7.5 ± 4.4
E_{a_5}	102 ± 52.7	109 ± 38.1	98.7 ± 38.2	$87.2 \pm \ldots$
k_{-5}	$3.9 \pm \ldots$	$2.7 \pm \ldots$	$7.1 \pm \ldots$	$1.1 \pm \ldots$
$E_{a_{-5}}$	151 ± 66.7	143 ± 17	118 ± 26	122 ± 71
k_6	21 ± 5.7	16.8 ± 2.6	$12.2 \pm \ldots$	18.8 ± 5.1
E_{a_6}	$67.7 \pm \ldots$	62.8 ± 10.2	68.9 ± 26.7	$72.2 \pm \ldots$
$-\Delta S_H$	144 ± 11.3	142 ± 8.7	141 ± 17.2	143 ± 47.7
$-\Delta H_H$	53.9 ± 1.1	56.8 ± 1.9	65.1 ± 17.9	68.6 ± 28.1
$-\Delta S_A$	67.1 ± 17	69.7 ± 9.4	71.9 ± 13.7	69.1 ± 26.2
$-\Delta H_A$	62.3 ± 1.2	62.4 ± 0.3	57.8 ± 22.7	58.2 ± 12
X	4.2 ± 1.5	3.9 ± 0.7	3.9 ± 1.9	4.1 ± 1.1
α			0.61 ± 0.3	0.63 ± 0.2

$\ldots$, Large standard error. The units are $k_i = [\,] \times 10^{-4}\ \mathrm{mol\,s^{-1}\,g_{metal}^{-1}}$, $E_i = [\,]\ \mathrm{kJ\,mol^{-1}}$, $\Delta S_i = [\,]\ \mathrm{J\,mol^{-1}\,K^{-1}}$, $\Delta H_i = [\,]\ \mathrm{kJ\,mol^{-1}}$.

distinguished. Slightly higher adsorption enthalpies for hydrogen are observed for the semicompetitive model, whereas the adsorption enthalpies for *o*-xylene adsorption are lower compared with the competitive adsorption model.

It can be safely concluded, however, that the parameters for the adsorption of the reactants are reliably estimated, giving reasonable values consistent with thermodynamic data. Thus, for hydrogen the entropy was calculated to be 142–144 J/(mol K), which is close to the gas-phase entropy of H_2 (130.7 J/mol K) [42]. For *o*-xylene the corresponding value was 67–72 J/(mol K). The estimated adsorption enthalpies for hydrogen were around −55 kJ/mol (competitive adsorption) and −62 to −65 kJ/mol (semicompetitive adsorption) and ∼ −62 kJ/mol (competitive adsorption) and −69 to −72 kJ/mol (semicompetitive) for *o*-xylene. In addition, heats of hydrogen adsorption have previously been measured calorimetrically on Pd/Al_2O_3 to be ∼ 73 kJ/mol [43], which is in relatively good agreement with the calculations.

The calculated activation energies for the first two steps, 116–135 kJ/mol, are consistent with the activation energies reported for aromatics hydrogenation. The values of E_{a_3}, E_{a_4}, and E_{a_6} (60–80 kJ/mol) are nearly equal. E_{a_6}, corresponding to the activation energy of *trans* formation, has a lower value than E_{a_4}, and the pre-exponential factors are very similar. This is reasonable, since the rate of *trans* formation is significantly larger than the rate of *cis* formation. The values of the rate constants k_4 and k_6 are much larger than the values of k_1 and k_2, which indicates that hydrogenation of an olefin (intermediate) is faster than the overall hydrogenation, corresponding well with the experimental data on the relative rates of aromatic and cycloalkene hydrogenation [14]. Furthermore, k_6 is higher than k_4, which means that O′ is hydrogenated faster than O.

A sensitivity analysis of some of the parameters for the competitive model in the form of contour plots is presented in Fig. 8. As can be seen, the correlation between the parameters is relatively low, although some correlation is visible for the parameters E_{a_3} and k_3. The values of ΔH_i and ΔS_i for adsorption were generally correlated to a greater extent with each other than they were to the values of E_{a_i} and k_i.

Finally, the estimated number of surface sites covered by the aromatic molecule (x in Table 1) is approximately 4, which seems to be reasonable, since *o*-xylene is a large molecule (compared with hydrogen) that is able to cover four sites. Let us compare this number with the data available from surface science measurements. The theoretical saturation coverage of benzene (corresponding to the maximum amount of benzene that can be accommodated in a flat-lying orientation) has been estimated from TPD and molecular beam measurements to be 0.14–0.16 ML on a Pd(111) surface [44–46], which corresponds to six or seven

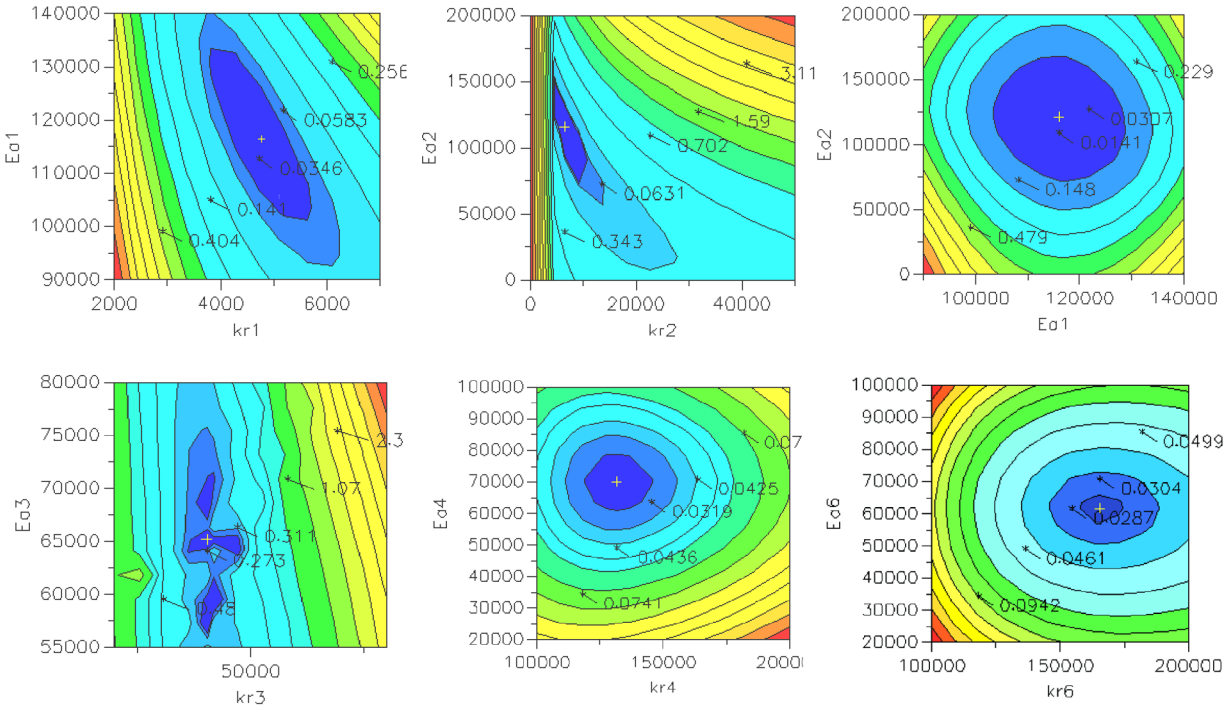

Fig. 8. Contour plots for parameters E_{a_1} vs. k_{r_1}, E_{a_2} vs. k_{r_2}, E_{a_2} vs. E_{a_1}, E_{a_3} vs. k_{r_3}, E_{a_4} vs. k_{r_4} and E_{a_6} vs. k_{r_6}. + is the reference point.

Pd atoms for each benzene molecule and a total coverage of 0.96. Orozco et al. [47] investigated the adsorption of another aromatic molecule, toluene, on Pd–alumina. The results for the amounts of hydrocarbon adsorbed to the catalyst expressed as the ratio of the number of hydrocarbon molecules to the number of surface metal atoms equal to 0.307 (e.g., ~ 3.3 Pd atoms/toluene molecule) at 523 K are in close agreement with the calculated values from the present study.

4. Conclusion

The kinetic modeling of gas-phase hydrogenation of *o*-xylene over Pd/Al_2O_3 was performed with different models based on elementary step mechanisms: competitive adsorption, noncompetitive adsorption, and semicompetitive adsorption between hydrogen and *o*-xylene. All models assumed multicentered adsorption of organic molecules. In contrast to previous reports in the literature, the model assuming competitive adsorption turned out to better explain the stereochemical product distribution. An extension of the competitive model (e.g., the semicompetitive model) was developed, taking into account that the organic molecule is not able to completely cover the surface of the catalyst because of the considerable difference in size between hydrogen and the aromatic molecule and geometrical restrictions. Hydrogen is thus able to adsorb on the interstitial sites between the organic molecules. This model, in addition to explaining stereoselectivity, was also able to capture the main kinetic regularities, such as an increase of reaction order in hydrogen with temperature, a slightly negative rate dependence on *o*-xylene, and the temperature dependence typical for hydrogenation of aromatic compounds, where the reaction rate passes through a maximum. Moreover, kinetic modeling resulted in physically reasonable values for the estimated parameters. The model considering competitive adsorption between hydrogen and organic molecules is preferred, from a statistical point of view, since the parameters estimated for the semicompetitive model are less accurate. The two models, however, are capable of describing the hydrogenation of *o*-xylene with almost the same degree of explanation.

References

[1] M. Viniegra, G. Córdoba, R. Gómez, J. Mol. Catal. 58 (1990) 107.
[2] G. Cordoba, J.L.G. Fierro, A. López-Goana, N. Martin, M. Viniegra, J. Mol. Catal. A 96 (1995) 155.
[3] N. Martin, G. Córdoba, A. López-Gaona, M. Viniegra, React. Kinet. Catal. 44 (1991) 381.
[4] S. Smeds, T. Salmi, D.Yu. Murzin, Appl. Catal. A 145 (1996) 253.
[5] S. Smeds, D. Murzin, T. Salmi, Appl. Catal. A 141 (1996) 207.
[6] S. Smeds, T. Salmi, D. Murzin, Appl. Catal. A 150 (1997) 115.
[7] M.A. Keane, J. Catal. 347 (1997) 166.
[8] M.A. Keane, P.M. Patterson, Ind. Eng. Chem. Res. 38 (1999) 1295.
[9] M.A. Keane, P.M. Patterson, J. Chem. Soc., Faraday Trans. 92 (1996) 1413.
[10] M.A. Aramendía, V. Borau, C. Jiménez, J.M. Marinas, F. Rodero, M.E. Sempre, React. Kinet. Catal. Lett. 46 (1992) 305.
[11] R.A. Saymeh, H.M. Asfour, Oriental J. Chem. 16 (2000) 67.
[12] R.A. Saymeh, H.M. Asfour, W.A. Tuaimen, Asian J. Chem. 9 (1997) 350.
[13] R.A. Saymeh, H.M. Asfour, W.A. Tuaimen, Indian J. Chem. 36B (1997) 799.

[14] S.D. Lin, M.A. Vannice, J. Catal. 143 (1993) 563.
[15] D.Yu. Murzin, N.A. Sokolova, N.V. Kul'kova, M.I. Temkin, Kinet. Katal. 30 (1989) 1352.
[16] M.I. Temkin, D.Yu. Murzin, N.V. Kul'kova, Kinet. Katal. 30 (1989) 637.
[17] J.W. Thybaut, M. Saeys, G.B. Marin, Chem. Eng. J. 90 (2002) 117.
[18] L.-P. Lindfors, T. Salmi, Ind. Eng. Chem. Res. 32 (1993) 34.
[19] S. Siegel, G.V. Smith, B. Dmuchovsky, D. Dubbel, W. Halpern, J. Am. Chem. Soc. 84 (1962) 3136.
[20] D. Murzin, S. Smeds, T. Salmi, React. Kinet. Catal. Lett. 60 (1997) 57.
[21] A. Kalantar Neyestanaki, P. Mäki-Arvela, H. Backman, H. Karhu, T. Salmi, J. Väyrynen, D.Yu. Murzin, J. Mol. Catal. A. 193 (2003) 237.
[22] A. Kalantar Neyestanaki, H. Backman, P. Mäki-Arvela, J. Wärnå, T. Salmi, D.Yu. Murzin, Chem. Eng. J. 91 (2003) 271.
[23] M. Saeys, M.-F. Reyniers, M. Neurock, G.B. Marin, J. Phys. Chem. B 109 (2005) 2064.
[24] M. Saeys, J.W. Thybaut, M. Neurock, G.B. Marin, Mol. Phys. 10 (2004) 267.
[25] M.I. Temkin, Kinet. Katal. 27 (1986) 533.
[26] S. Smeds, T. Salmi, D.Yu. Murzin, React. Kinet. Catal. Lett. 63 (1998) 47.
[27] D.E. Wilk, C.D. Stanners, Y.R. Shen, G.A. Somorjai, Surf. Sci. 280 (1993) 298.
[28] B.E. Koel, D.A. Blank, E.A. Carter, J. Mol. Catal. A 131 (1998) 39.
[29] Y. Inuone, J.M. Herrmann, H. Schmidt, R.L. Burwell, J.B. Butt, J.B. Cohen, J. Catal. 53 (1978) 401.
[30] D.Yu. Murzin, Recent Res. Devel. Catal. 2 (2003) 143.
[31] S. Siffert, D.Yu. Murzin, F. Garin, Appl. Catal. A 178 (1999) 89.
[32] A. Frennet, G. Lienard, A. Grucq, L. Degols, J. Catal. 46 (1975) 1.
[33] D. Murzin, S. Salmi, S. Smeds, M. Laatikainen, M. Mustonen, E. Paatero, React. Kinet. Catal. Lett. 61 (1997) 227.
[34] J.-P. Mikkola, H. Vainio, T. Salmi, R. Sjöholm, T. Ollonqvist, J. Väyrynen, Appl. Catal. A 196 (2000) 143.
[35] W.H. Press, B.P. Flannery, S.A. Teukolsky, W.T. Vetterling, Numerical Recipes: The Art of Scientific Computing, Cambridge University Press, Cambridge, 1990.
[36] H. Haario, MODEST 6.0-User's Guide, Profmath Oy, Helsinki, 2001.
[37] R. Hudges, Deactivation of Catalysts, Academic Press, London, 1984.
[38] M. Consonni, R. Toroude, D.Yu. Murzin, Chem. Eng. Technol. 21 (1998) 605.
[39] R.L. Motard, R.F. Burke, L.N. Canjar, R. Beckmann, J. Appl. Chem. 7 (1957) 1.
[40] L.-P. Lindfors, T. Salmi, S. Smeds, Chem. Eng. Sci. 48 (1993) 3813.
[41] Yu.S. Snagovskii, Zh. Fiz. Khim. 46 (1972) 2367.
[42] D.R. Liede (Ed.), CRC Handbook of Chemistry and Physics, CRC Press, Boca Raton, FL, 2004.
[43] P. Chou, M.A. Vannice, J. Catal. 104 (1987) 1.
[44] W.T. Tysoe, R.M. Ormerod, R.M. Lambert, G. Zgrablich, A. Ramirez-Cuesta, J. Phys. Chem. 97 (1993) 3365.
[45] A.F. Lee, K. Wilson, R.M. Lambert, A. Goldoni, A. Baraldi, G. Paolucci, J. Phys. Chem. B 104 (2000) 11729.
[46] F. Mittendorfer, C. Thomazeau, P. Raybaud, H. Toulhoat, J. Phys. Chem. B 107 (2003) 12287.
[47] J.M. Orozco, G. Webb, Appl. Catal. 6 (1983) 67.